

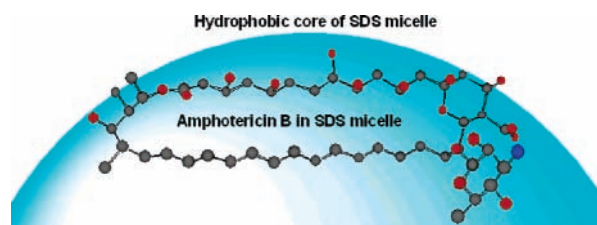
## Conformation and Position of Membrane-Bound Amphotericin B Deduced from NMR in SDS Micelles

Nobuaki Matsumori,\* Toshihiro Houdai, and Michio Murata\*

Department of Chemistry, Graduate School of Science, Osaka University, Machikaneyama, Toyonaka, Osaka 560-0043, Japan

murata@ch.wani.osaka-u.ac.jp; matsumori@ch.wani.osaka-u.ac.jp

Received June 26, 2006



Amphotericin B (AmB) is known to self-assemble to form an ion channel across lipid bilayer membranes. To gain insight into the conformation of AmB in lipidic environments, AmB in SDS micelles was subjected to high-resolution NMR and CD measurements, and the NMR-derived conformation thus obtained was refined by molecular mechanics calculations. These results indicate that AmB in SDS micelles is conformationally fixed particularly for the macrolide moiety. Paramagnetic relaxation experiments with the use of  $Mn^{2+}$  reveal that AmB is shallowly embedded in the micelle with the polyhydroxyl chain being close to the water interface and the side of polyene portion facing to the micelle interior. CD measurements demonstrate that AmB is in a monomeric form in SDS micelles. The structure of AmB in the micelles obtained in the present study may reproduce the initial stage of membrane interaction of AmB prior to the assembly formation in biomembranes.

### Introduction

For over 40 years, amphotericin B (AmB) has been a standard drug for treatment of deep-seated systemic fungal infections.<sup>1–3</sup> Due to the lack of better alternatives as well as the infrequent occurrence of resistant strains,<sup>4</sup> AmB is still an important drug. It is generally accepted that AmB associates with sterols to form a barrel-stave pore in phospholipid membranes, with the polyhydroxy side pointing inward and the lipophilic heptaene

part facing outward.<sup>5,6</sup> The occurrence of such molecular assemblies in fungal plasma membrane increases permeability to ions, ultimately leading to cell death.<sup>6–9</sup> The pharmacological action of AmB is based on its selective toxicity against eukaryotic microbes over mammals; ergosterol-containing fungal membranes are more sensitive to AmB than cholesterol-containing mammalian ones.<sup>8,10,11</sup> Consequently, the concentra-

\* Corresponding authors. Tel: +81-6-6850-5774 (M.M.), +81-6-6850-5569 (N.M.). Fax: +81-6-6850-6785.

(1) Gallis, H. A.; Drew, R. H.; Pickard, W. W. *Rev. Infect. Dis.* **1990**, *12*, 308–329.

(2) Hartsel, S. C.; Bolard, J. *Trends Pharmacol. Sci.* **1996**, *12*, 445–449.

(3) Ablordeppey, S. Y.; Fan, P. C.; Ablordeppey, J. H.; Mardenborough, L. *Curr. Med. Chem.* **1999**, *6*, 1151–1195.

(4) Vanden-Bossche, H.; Dromer, F.; Improvisi, I.; Lozano-Chiu, M.; Rex, J. H.; Sanglard, D. *Med. Mycol.* **1998**, *36*, 119–128.

(5) Andreoli, T. E. *Ann. New York Acad. Sci.* **1974**, *235*, 448–468.

(6) De-Kruijff, B.; Demel, R. A. *Biochim. Biophys. Acta* **1974**, *339*, 57–70.

(7) Cohen, B. E. *Biochim. Biophys. Acta* **1986**, *857*, 117–122.

(8) Vertut-Croquin, A.; Bolard, J.; Chabbert, M.; Gary-Bobo, C. *Biochemistry* **1983**, *22*, 2939–2944.

(9) Van-Hoogevest, P. De-Kruijff, B. *Biochim. Biophys. Acta* **1978**, *511*, 397–407.

(10) Milhau, J.; Hartman, M. A.; Bolard, J. *Biochim.* **1989**, *71*, 49–56.

(11) Vertut-Croquin, A.; Bolard, J.; Gary-Bobo, C. M. *Biochem. Biophys. Res. Commun.* **1984**, *125*, 360–366.

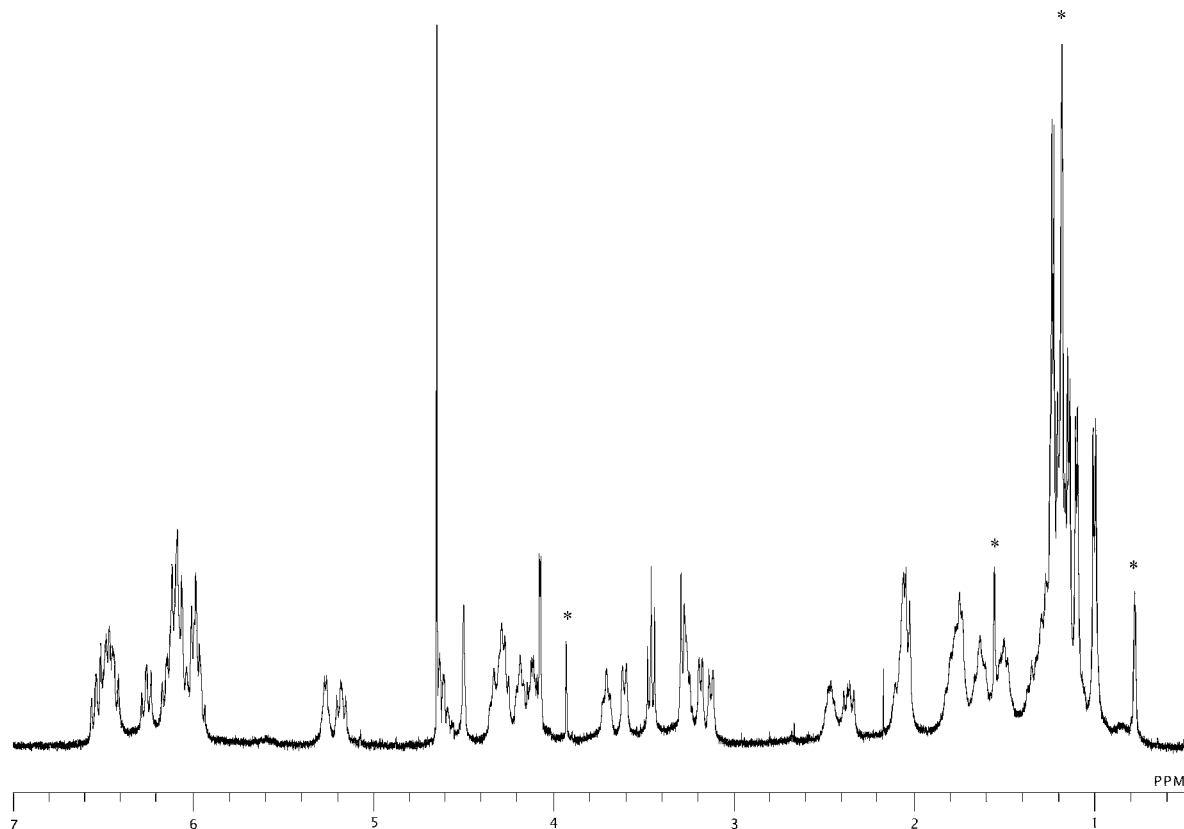
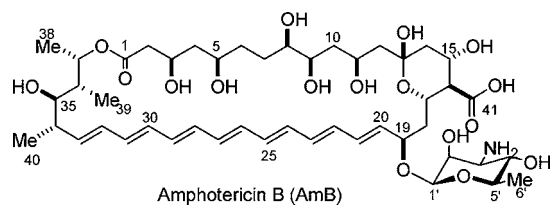


**FIGURE 1.** 500 MHz  $^1\text{H}$  NMR spectrum of AmB (5 mM) in SDS- $d_{25}$  (75 mM) and  $\text{D}_2\text{O}$  at 30  $^\circ\text{C}$ . The water signal was suppressed with a DANTE sequence. \*Signals derived from residual protons of SDS- $d_{25}$ .

tion of AmB necessary to elicit the lethal permeability is higher in biomembranes with cholesterol than those with ergosterol.

The structure of AmB is comprised of two conformationally rigid parts, a macrolide ring and a mycosamine sugar moiety, which are linked by a rotatable  $\beta$ -glycosidic bond. Their relative position is thought to control AmB–AmB and AmB–sterol interactions, where inter- and intramolecular hydrogen bonds play crucial roles.<sup>12,13</sup> We have recently prepared the conformation-restricted derivatives of AmB, in which carboxyl and amino groups are bridged with various lengths of alkyl chain,<sup>14</sup> and revealed that the amino-sugar orientation strongly affects the ergosterol-selectivity in membrane-permeabilizing activity. In this paper, to gain further insight into the structural properties of AmB in amphiphilic environments, the conformation and binding mode of AmB were examined in SDS micelles on the basis of NMR, CD and molecular mechanics calculations.



(12) Baginski, M.; Gariboldi, P.; Bruni, P.; Borowski, E. *Biophys. Chem.* **1997**, *65*, 91–100.

(13) Baginski, M.; Resat, H.; Borowski, E. *Biochim. Biophys. Acta* **2002**, *1567*, 63–78.

(14) Matsumori, N.; Sawada, Y.; Murata, M. *J. Am. Chem. Soc.* **2005**, *127*, 10667–10675.

## Results and Discussion

**Conformation of Amphotericin B in SDS Micelles.** The NMR sample was prepared by mixing 5 mM AmB and 75 mM SDS- $d_{25}$  in  $\text{D}_2\text{O}$  to give a clear suspension. The NMR spectrum of the solution (Figure 1) gave rise to high-resolution signals of AmB, which is possibly due to the rapid lateral diffusion of AmB in SDS micelles as well as to the fast reorientation of the micelles. The  $^1\text{H}$  chemical shifts were fully assigned on the basis of COSY and NOESY spectra (Table 1). The amino group of AmB was found to be protonated in SDS micelles because the 3'-H and neighboring resonances were shifted higher frequency in the micelles from those in DMSO (Table 1). Then, to gain information on the ionization state of the carboxyl group of AmB, we measured the  $^{13}\text{C}$  NMR spectra of AmB in SDS micelles using uniformly  $^{13}\text{C}$ -labeled AmB.<sup>15</sup> The chemical shifts of the AmB carboxyl group were found to be 175.5 ppm in DMSO- $d_6$  and 178.5 ppm in SDS micelles. For comparison, we also measured  $^{13}\text{C}$  NMR of propionic acid in DMSO- $d_6$ , in 1 M NaOH- $\text{D}_2\text{O}$ , and in 1 M HCl- $\text{D}_2\text{O}$ . The shift of C1 of propionic acid was 174.9 ppm in DMSO- $d_6$ , 183.9 ppm in NaOH- $\text{D}_2\text{O}$ , and 178.6 ppm in HCl- $\text{D}_2\text{O}$ . The comparison of  $^{13}\text{C}$  chemical shifts suggests that the carboxyl group of AmB is hardly ionized in SDS micelles. The pH of the suspension prepared by the same method as the NMR sample except that  $\text{H}_2\text{O}$  was used instead of  $\text{D}_2\text{O}$  was 7.1, at which the carboxyl group of AmB was supposed to be ionized. To explain the unionization of the carboxyl group of AmB in the micelle, we should take account of negative charges of the micelle surface

(15) Matsuoka, S.; Ikeuchi, H.; Umegawa, Y.; Matsumori, N.; Murata, M. *Bioorg. Med. Chem.* **2006**, *14*, 6608–6614.

**TABLE 1.** <sup>1</sup>H Chemical Shifts (ppm) of AmB in SDS Micelles and in a DMSO Solution

position	SDS micelle <sup>a</sup>		position	DMSO <sup>b</sup>	
	micelle <sup>a</sup>	DMSO <sup>b</sup>		micelle <sup>a</sup>	DMSO <sup>b</sup>
2	2.04, 2.35	2.16	22	6.48	
3	4.18	4.05	23, 25, 27	6.05–6.15	
4	1.21, 1.51	1.32, 1.38	24, 26	6.45–6.55	
5	3.70	3.51	28	6.44	6.0–6.5
6	1.22, 1.49	1.24, 1.40	29	6.06	
7	1.25, 1.75	1.24, 1.58	30	6.26	
8	3.13	3.09	31	5.99	
9	3.61	3.46	32	6.15	6.08
10	1.25, 1.76	1.30, 1.56	33	5.18	5.42
11	4.33	4.24	34	2.46	2.27
12	1.61, 1.80	1.57	35	3.18	3.08
14	1.34, 2.04	1.09, 1.83	36	1.74	1.71
15	4.11	3.97	37	5.26	5.20
16	2.04	1.82	38	1.14	1.10
17	4.27	4.17	39	1.00	0.90
18	1.64, 2.08	1.48, 2.14	40	1.10	1.03
19	4.28	4.39	1'	4.50	4.50
20	6.02	5.96	2'	4.08	3.71
21	5.97	6.10	3'	3.29	2.76
			4'	3.45	3.14
			5'	3.26	3.24
			6'	1.22	1.16

<sup>a,b</sup> Conditions: 5 mM AmB in SDS-*d*<sub>25</sub> 75 mM and D<sub>2</sub>O at 30 °C and 10 mM AmB in DMSO-*d*<sub>6</sub> at 25 °C, respectively.

**TABLE 2.** Apparent Vicinal Coupling Constants of AmB in SDS Micelles and in DMSO

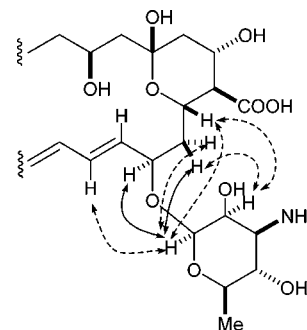
coupled protons <sup>a</sup>	coupling value <sup>b</sup> (Hz)		coupled protons <sup>a</sup>	coupling value <sup>b</sup> (Hz)	
	SDS micelle	DMSO		SDS micelle	DMSO
2 <sup>h</sup> , 3	10	n.d. <sup>c</sup>	17, 18 <sup>l</sup>	10	10
3, 4 <sup>h</sup>	10	n.d. <sup>c</sup>	18 <sup>l</sup> , 19	2–3	2–3
4 <sup>h</sup> , 5	10	9	18 <sup>h</sup> , 19	2–3	2–3
5, 6 <sup>h</sup>	10	9	19, 20	9	8
7 <sup>h</sup> , 8	11	10	32, 33	13	14
8, 9	<1	<1	33, 34	10	11
9, 10 <sup>h</sup>	11	10	34, 35	10	10
10 <sup>h</sup> , 11	10	10	35, 36	<1	<2
11, 12 <sup>h</sup>	10	10	36, 37	~1	~1

<sup>a</sup> *h*: a higher frequency proton of a geminal pair in methylene. *l*: a lower frequency proton. <sup>b</sup> Data have a maximum of 0.8 Hz error due to the digital resolution of DQF-COSY. <sup>c</sup> Coupling constants were not determined due to strong secondary effects from merged methylene signals at H-2 and H-4.

due to the anionic nature of SDS sulfate. Under the negative potential, p*K*<sub>a</sub> values of carboxylic acids are known to increase.<sup>16</sup> Since the carboxyl group of AmB is localized close to the micelle surface as described below, the surface negative potential of SDS micelles is thought to prevent the ionization of the carboxyl group even under neutral pH conditions. As we reported previously,<sup>15</sup> the chemical shift of C41 of AmB in DMPC dispersion agreed well with the present value in SDS micelles, implying the un-ionized carboxylic acid in lipid layer membranes.

We could obtain a significant number of vicinal coupling constants in the macrolactone part from one-dimensional <sup>1</sup>H and DQF-COSY spectra (Table 2). All the coupling constants measured in SDS micelles are typical for *anti* or *gauche* orientations, which denotes that the macrolide portion of AmB is conformationally rigid under the micelle conditions. In addition, dihedral angles deduced from the coupling data are

(16) Fernández, M. S.; Fromherz, P. *J. Phys. Chem.* **1977**, *81*, 1755–1761.

**FIGURE 2.** Long-range NOEs between the sugar portion and macrolide in SDS micelles. The solid and dashed arrow-headed lines represent strong and weak NOEs, respectively.

consistent with those in the crystal structure of *N*-iodoacetyl derivative of AmB,<sup>17</sup> suggesting conformational similarity in the macrolide portion to the crystal structure. These features for the macrolide ring were further supported by reasonably observed transannular NOEs between H-3,5,9,11 and heptaene protons (Figure S9, Supporting Information).

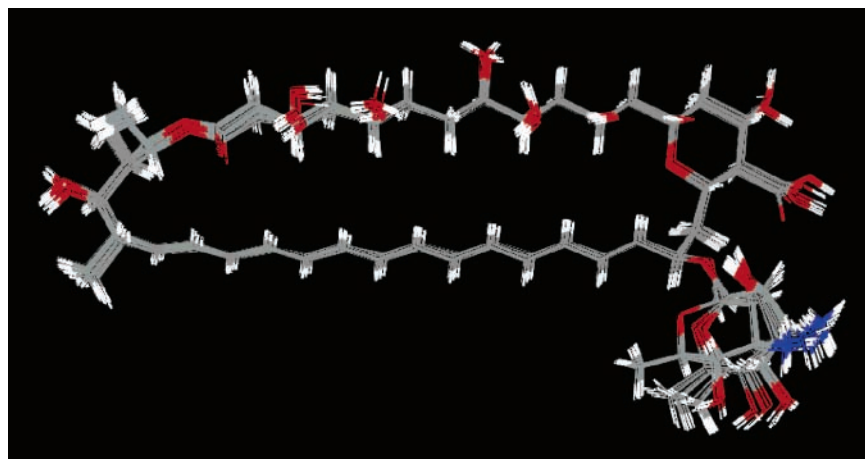
The orientation of the sugar moiety with respect to the macrolide ring in SDS micelles was determined on the basis of NOE data. Relevant NOEs of AmB in the micelles around the sugar, most of which are also observed in AmB in DMSO, are illustrated in Figure 2. To get a more precise picture of AmB in the micelles, we carried out molecular modeling using the Monte Carlo conformational search algorithm<sup>18</sup> with the aid of the seven NOE constraints shown in Figure 2, which were divided into two groups with upper distance limits of 3.3 and 4.5 Å based on NOE intensities in comparison with rigid standard values among the aminosugar signals (Figure 2). Due to the immobility of the macrolide ring and the conformational similarity to the crystal structure as described above, this part was treated as a motion-restricted portion, where ±30° allowance from the crystal structure<sup>17</sup> was given to each C–C single bond upon calculation. A continuum solvation model using a generalized Born-surface area (GB/SA) method was applied for water through the calculation because most part of AmB molecule except the heptaene is likely in water-accessible region of the SDS micelle as estimated below. Under these conditions, 1000 random conformers were generated and subjected to energy minimization by the conjugate gradient method.

Figure 3 shows a superposition of 50 lowest energy conformations of AmB in SDS micelles within 2.1 kcal mol<sup>-1</sup>. The conformers have some flexibility in the glycoside bonds, but the other possible conformer, where 2'-OH and 41-COOH are hydrogen-bonded, was found to be energetically unfavorable. The φ (C18–C19–O–C1') and ψ (C19–O–C1'–C2') angles of the lowest energy conformer were determined to be -92.0° and 165.6°, respectively. The conformational preference of the ψ angle can be explained by the exo-anomeric effect for β-anomers.<sup>19</sup> We have previously prepared the conformationally restricted derivatives of AmB by bridging the amino and carboxyl groups with various lengths of chains, and determined the conformation of the derivative that showed the highest

(17) Ganis, P.; Avitabile, G.; Mechlini, W.; Schaffner, C. P. *J. Am. Chem. Soc.* **1971**, *93*, 4560–4564.

(18) Charbonneau, C.; Fournier, I.; Dufresne, S.; Barwicz, J.; Tancrede, P. *Biophys. Chem.* **2001**, *91*, 125–133.

(19) Bitzer, R. S.; Barbosa, A. G. H.; da Silva, C. O.; N., Marco A. C. *Carbohydr. Res.* **2005**, *340*, 2171–2184.



**FIGURE 3.** Superposition of 50 lowest energy conformations of AmB in SDS micelles within 2.1 kcal/mol, which were generated by the Monte Carlo algorithm restrained with distance constraints from NOEs. Models are superposed for the minimum rmsd (similar conformations with respect to the glycoside bonds were obtained without the NOE constraints).

**TABLE 3.**  $T_1^0$ ,  $T_{1P}$ , and  $T_{1M}$  Values of  $^1\text{H}$  NMR Signals of AmB in SDS Micelles in the Presence of  $30\ \mu\text{M}$   $\text{Mn}^{2+}$

position	$T_1^0$ (ms)	$T_{1P}^a$ (ms)	$T_{1M}^a$ (ms)	position	$T_1^0$ (ms)	$T_{1P}^a$ (ms)	$T_{1M}^a$ (ms)
2 <sup>b</sup>	926	370	615	34	1051	429	726
3	1220	354	498	35	908	503	1126
5	1229	324	440	37	1359	419	606
8	1486	492	737	38	690	308	558
9	1352	573	994	39	611	323	684
15	1780	322	394	40	1181	418	647
21, 23, 25, 27, 29, 31	2596	1176	2151	1'	1345	216	257
22, 24, 26, 28	2241	770	1173	4'	1788	625	962
33	1719	801	1500	6'	639	436	1375

<sup>a</sup> Data may have errors up to 10%. <sup>b</sup> Higher frequency protons of the methylene at C2.

ergosterol-selectivity on the basis of distance and dihedral constraints obtained in a DMSO solution.<sup>14</sup> The  $\varphi$  and  $\psi$  angles in the most stable conformer were determined to be  $-89.3^\circ$  and  $153.8^\circ$ , respectively, which are very close to the current data. This conformational consistency between AmB in micelles and the derivative suggests that the simulated structure shown in Figure 3 may represent the active conformation of AmB in membrane environments.

**Position of Amphotericin B in SDS Micelles.** Paramagnetic ions such as  $\text{Mn}^{2+}$  have long been used for estimating the depth of bound entities in micelles.<sup>20</sup> Relaxation induced by  $\text{Mn}^{2+}$  shows how observed nuclei are close to the aqueous interface of micelles. The paramagnetic contribution to the spin–lattice relaxation is represented by  $T_{1M}$

$$\frac{1}{T_{1M}} = \frac{1}{T_{1P}} - \frac{1}{T_1^0}$$

where  $T_1^0$  and  $T_{1P}$  are spin–lattice relaxation times in the absence and presence of  $\text{Mn}^{2+}$ , respectively.<sup>21</sup> Paramagnetic relaxation time  $T_{1M}$  has explicit  $r^{-6}$ -distance dependency, which makes it possible to measure semiquantitatively the depth of a micelle-bound entity; the  $T_{1M}$  values of the hydrogen atoms at C1, C2, C3–C11, and C12 of non-deuterated SDS were 152, 390, 1128, and 1101 ms, respectively, demonstrating that C1

and C2 portions of SDS are accessible to  $\text{Mn}^{2+}$ . Then we measured  $T_{1M}$  values of  $^1\text{H}$  signals of AmB in SDS micelles in the presence of  $30\ \mu\text{M}$   $\text{Mn}^{2+}$  (Table 3), though we could not determine all of the  $T_{1M}$  values of AmB due to not only signal overlap on 1D  $^1\text{H}$  NMR spectra but signal broadenings by the addition of  $\text{Mn}^{2+}$ . Apparently,  $\text{Mn}^{2+}$  strongly influences protons at the C2–C15 polyhydroxyl chain of AmB (Table 3), and their  $T_{1M}$  values are roughly comparable to that of C2 of SDS, which indicates that the chain resides close to the micelle surface. Interestingly, the relaxation profiles for the polyhydroxyl portion are slightly different among hydroxyl-bearing methine protons; terminal H-2, -3, -5, and -15 are more effectively relaxed with  $\text{Mn}^{2+}$  than H-8 and H-9 residing in the central part. This may be accounted for by the notion that H-8 and -9 are more distant from the surface due to the high curvature of the micelle.

Similarly, the low  $T_{1M}$  values of C38, C39, and C40 methyl protons, which are located at one end of the molecule, reveal their vicinity to the micelle surface. The  $T_{1M}$  values of the sugar moiety also suggest that H-1' is in close vicinity to the water-micelle interface, while methyl protons at C6' are rather distant from the surface. As described above, the amino group of AmB is ionized under these conditions, suggesting its electrostatic interaction with the sulfate group of SDS in the water-accessible region.

The larger  $T_{1M}$  values observed for the heptaene protons (H-20–H-33) suggest their deeper immersion into the micelle interior. Among those, hydrogen atoms on odd-numbered carbons have lower frequency chemical shifts while those on even-numbered carbons give rise to higher frequency signals by around 0.5 ppm (Table 1). The difference in chemical shift

(20) (a) Palian, M. M.; Boguslavsky, V. I.; O'Brien, D. F.; Polt, R. J. *Am. Chem. Soc.* **2003**, *125*, 5823–5831. (b) Whaley, W. L.; Rummel, J. D.; Kastropeli, N. *Langmuir* **2006**, *22*, 7175–7184. (c) Lindberg, M.; Jarvet, J.; Langel, Ü.; Gräslund, A. *Biochemistry* **2001**, *40*, 3141–3149.

(21) Villalain, J. *Eur. J. Biochem.* **1996**, *241*, 583–593.



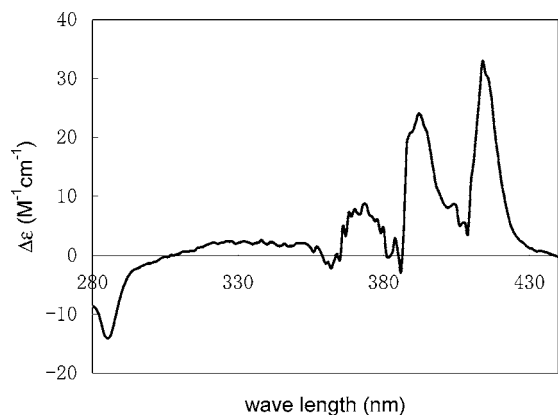


FIGURE 4. CD spectrum of 0.5 mM AmB in 8 mM SDS solution.

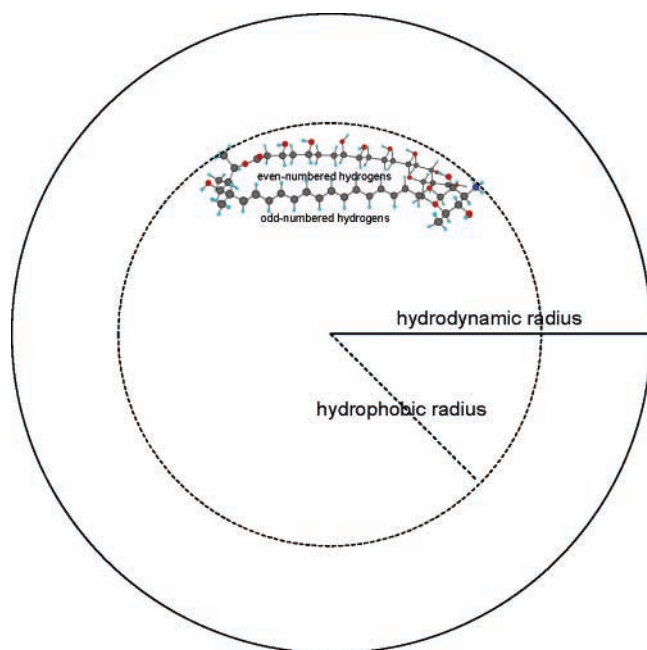


FIGURE 5. Schematic illustration of AmB placed in an SDS micelle with 30 Å hydrodynamic and 20 Å hydrophobic radii according to the self-diffusion coefficients as described in the text. The conformation and location of AmB are based on the current data.

can be accounted for by the transannular deshielding effects of oxygen atoms that come close to the even-numbered hydrogens on the heptaene as depicted in Figures 3 and 5.<sup>22</sup> Longer  $T_{1M}$  values for the odd protons (Table 3) reveal that this side of the polyene chain faces to the micelle interior, and relatively shorter  $T_{1M}$  values for the even protons indicate that the other side of the polyene is closer to the micelle–water interface (Figure 5).

**Size of SDS Micelles in the Presence and Absence of Amphotericin B.** We examined the size of SDS micelles in the presence and absence of AmB on the basis of diffusion coefficients determined by PFG-STE NMR experiments.<sup>23</sup> The observed diffusion coefficient for 72 mM SDS in the absence of AmB was  $1.05 \times 10^{-10} \text{ m}^2 \text{ s}^{-1}$ , which agreed well with the

reported values ( $\sim 0.92 \times 10^{-10} \text{ m}^2 \text{ s}^{-1}$ ).<sup>24</sup> Upon introduction of 4.5 mM AmB to the micelle, the diffusion coefficient was substantially reduced to  $0.77 \times 10^{-10} \text{ m}^2 \text{ s}^{-1}$ , indicating an increase in micelle size. The hydrodynamic radius of diffusing species,  $R_h$ , is inversely proportional to the self-diffusion coefficient  $D$  according to the Stokes–Einstein equation:

$$R_h = kT/6\pi\eta D \quad (\eta: \text{solution viscosity})$$

The reported hydrodynamic radius of an SDS micelle is 22.8 Å,<sup>25</sup> and therefore, the apparent hydrodynamic radius for the SDS micelle containing AmB is estimated to be around 30 Å, assuming that the viscosity of micelle suspensions is not affected by AmB and the micelles remain spherical. It is reported that the addition of salts or cationic surfactant to SDS dispersions induces the morphological changes of the micelles such as the transition from spherical to ellipsoidal or rod-like micelles.<sup>26</sup> However, these transitions result in a significant reduction in the diffusion coefficient by an order of magnitude. Therefore, the observed diffusion coefficient of SDS micelles in the presence of AmB is thought to fall in the range of globular micelles. Alternatively, even if the transition in micelle shape occurs, the extent of the transition should be relatively small, and the shape of the micelle can largely be regarded as the sphere.

The number of SDS molecules in a micelle is reported to be about 60,<sup>25</sup> and the AmB/SDS molar ratio in the present study is 1/15. Therefore, if the number of SDS molecules per micelle is unchanged, about 4 AmB molecules are incorporated in a micelle. As mentioned above, the addition of AmB resulted in the enlargement of micelle radius by more than 30%, which corresponded to the swelling of volume more than twice. Assuming that the micelle volume is approximately proportional to the total of molecular weights in a micelle, the incorporation of 4 molecules of AmB in a micelle would result in an increase in volume just by 20%, which cannot explain the doubling of micelle volume. Therefore, it might be more plausible that AmB reduces electrostatic repulsion and tightens the packing of head groups of SDS, hence resulting in a decrease in the micelle curvature and thus an increase in the number of aggregated SDS molecules per micelle.

**Orientation of Monomeric Amphotericin B in Micelles Implying Its Binding to the Membrane.** We next recorded the CD spectrum of AmB in SDS micelles to know whether AmB forms aggregates in the micelles. AmB is known to give rise to a strong excitonic dichroic doublet centered at 340 nm upon aggregation.<sup>27</sup> As depicted in Figure 4, however, AmB did not show any dichroic splitting under the condition of 0.5 mM AmB and 8 mM of SDS (almost equal to the critical micelle concentration of SDS 8 mM<sup>28</sup>), indicating that AmB is mostly present as a monomeric form in SDS micelles. Since the critical micelle concentration of SDS is close to the concentration of the CD measurements, we also measured CD spectra at higher

(24) Orfi, L.; Lin, M.; Larive, C. K. *Anal. Chem.* **1998**, *70*, 1339–1345. Chen, W.-J.; Chen, S.-F.; Chang, D.-K. *Anal. Biochem.* **1998**, *264*, 211–215.

(25) Gao, X.; Wong, T. C. *Biophys. J.* **1998**, *74*, 1871–1888.

(26) (a) Hassan, P. A.; Raghavan, S. R.; Kaler, E. W. *Langmuir* **2002**, *18*, 2543–2548. (b) Hassan, P. A.; Sawant, S. N.; Bagkar, N. C.; Yakhmi, J. V. *Langmuir* **2004**, *20*, 4874–4880.

(27) Bolard, J.; Legrand, P.; Heitz, F.; Cybulska, B. *Biochemistry* **1991**, *30*, 5707–5715. Fujii, G.; Chan, J.-E.; Coley, T.; Steere, B. *Biochemistry* **1997**, *36*, 4959–4968.

(28) Johnson, C. S., Jr. *J. Magn. Reson. A* **1993**, *102*, 214–218.

(22) Abraham, R. J.; Byrne, J. J.; Griffiths, L.; Koniotou, R. *Magn. Reson. Chem.* **2005**, *43*, 611–624.

(23) Tanner, J. E. *J. Chem. Phys.* **1970**, *52*, 2523–2526.

AmB and SDS concentrations to ensure the micelle formation; 1 mM AmB and 16 mM SDS; 2 mM AmB and 32 mM SDS; and 0.5 mM AmB and 16 mM SDS in H<sub>2</sub>O. Although the CD spectra for 1 mM and 2 mM AmB solutions were in higher noise level due to the high UV absorption, the split cotton at 340 nm was not observed at any concentrations (data not shown), further supporting that AmB is present in a monomeric form under the conditions of the CD experiments.

Figure 5 illustrates the positioning of AmB relative to an SDS micelle. The figure also shows the approximate hydrodynamic radius (30 Å) of an AmB-bound SDS micelle and that of the hydrophobic core, the latter of which is generally smaller by 10 Å.<sup>29</sup> The size of the micelle is large enough to incorporate an AmB molecule. As described above, the polyhydroxyl chain of AmB resides at the water/micelle interface with the even-carbon side of the polyene portion facing to the surface. The cartoon in Figure 5 raises the question of how the three-dimensional structure in an SDS micelle may correlate with that in real biomembranes. Both micelles and bilayer membranes are composed of amphiphilic constituents, although their morphologies are quite different. Since it is repeatedly suggested that micelles do not always mimic bilayer membranes due to their high curvature,<sup>30</sup> extrapolation of the current results toward the AmB-bilayer interaction may not be straightforward. Indeed, we have shown that AmB can penetrate DMPC bilayer membrane with a single molecular length possibly upon ion channel formation,<sup>31</sup> which seems inconsistent with the present results. The estimated micelle diameter of ca. 60 Å is substantially larger than thickness of biological membranes, thus preventing AmB from spanning the micelle with single molecular length. Moreover, the surface negative charge of SDS micelles may also hamper aggregation of AmB. AmB is reported to be predominantly monomeric and horizontally embedded in a phospholipid membrane at low AmB/lipid ratios below 1 mol %.<sup>32</sup> In this respect, the structure of AmB in SDS micelles may represent an initial stage of membrane association of AmB from an aqueous phase toward the ion-channel formation in biological membranes.

In the recent decade, solid-state NMR techniques have greatly advanced and have been applied to membrane-bound AmB,<sup>15,31,33,34</sup> which have provided invaluable information on mobility and intermolecular distances. However, this approach demands not only specialized instruments but also extensive efforts in sample preparation involving specific isotopic labeling. In this respect, the use of micelles is an option for structure studies of membrane-bound AmB and other membrane-associated drugs, which would provide complementary information that is difficult to obtain only from solid-state NMR.

(29) Bruce, C. D.; Senapati, S.; Berkowitz, M. L.; Perera, L.; Forbes, M. D. E. *J. Phys. Chem. B* **2002**, *106*, 10902–10907.

(30) (a) Chou, J. J.; Kaufman, J. D.; Stahl, S. J.; Wingfield, P. T.; Bax, A. *J. Am. Chem. Soc.* **2002**, *124*, 2450–2451. (b) Lindberg, M.; Biverstahl, H.; Gräslund, A.; Mäler, L. *Eur. J. Biochem.* **2003**, *270*, 3055–3063.

(31) Matsuoka, S.; Ikeuchi, H.; Matsumori, N.; Murata, M. *Biochemistry* **2005**, *44*, 704–710.

(32) (a) Herec, M.; Dziubinska, H.; Trebacz, K.; Morzycki, J. W.; Gruszecki, W. I. *Biochem. Pharmacol.* **2006**, *70*, 668–675. (b) Gagos, M.; Gabrielska, J.; Dalla Serra, M.; Gruszecki, W. I. *Mol. Memb. Biol.* **2005**, *22*, 433–442.

(33) Hing, A. W.; Schaefer, J.; Kobayashi, G. S. *Biochim. Biophys. Acta* **2000**, *1463*, 323–332.

(34) Matsumori, N.; Sawada, Y.; Murata, M. *J. Am. Chem. Soc.* **2006**, *128*, 11977–11984.

## Conclusion

In the present study, we have deduced the 3D structure and position of AmB in SDS micelles. The conformation of AmB macrolide is rigid in the micelles, and the orientation of the sugar was similar to that of a conformationally restricted derivative of AmB with high ergosterol selectivity.<sup>14</sup> The stability of AmB in the micelle suggests that the orientation of the sugar moiety and the macrolide conformation closely mimic the active 3D structure of membrane-bound AmB. The paramagnetic relaxation experiments using Mn<sup>2+</sup> ion revealed that AmB is shallowly immersed in the micelle, with the polyhydroxyl chain close to the water interface and the polyene directed to the micelle interior. The monomeric nature of AmB in the micelle was shown by the CD spectrum. These results clearly demonstrate that monomeric AmB has a rigid conformation for the macrolide ring and possesses a particular aminosugar orientation with respect to the macrolide under amphiphilic conditions. These findings provide significant information as a guide for future investigations on the initial membrane binding of AmB leading to its antibiotic activity.

## Experimental Section

**NMR Measurements.** For a DMSO solution, AmB was dissolved under dry argon in DMSO-*d*<sub>6</sub> at 10 mM concentration. In SDS micelles, 5 mM AmB and 75 mM SDS-*d*<sub>25</sub> were suspended in D<sub>2</sub>O and shaken vigorously. This solution was quite stable for more than a week at room temperature and gave rise to reproducible NMR spectra. All NMR spectra were recorded at 30 °C on a 500 MHz spectrometer. The COSY spectrum was obtained as a matrix of 256 (*F*<sub>1</sub>) × 1024 (*F*<sub>2</sub>) complex data points. The DQF-COSY and NOESY spectra were recorded with a 1.5 s recovery delay in the phase-sensitive mode using the States method.<sup>35</sup> The number of data points was 1024 in the *F*<sub>2</sub> dimension and 128 in the *F*<sub>1</sub> dimension for NOESY and 4K (*F*<sub>2</sub>) by 256 (*F*<sub>1</sub>) for DQF-COSY. The spectral width in both dimensions was typically 3300 Hz. The data were processed using Alice2 version 4.1 (JEOL DATUM) and apodized with 40°-shifted square sine-bell window functions in both *F*<sub>1</sub> and *F*<sub>2</sub> dimensions for DQF-COSY and NOESY, and a sine-bell function was applied for COSY. The NOESY spectrum was recorded with a mixing time of 300 ms. In all the two-dimensional spectra for SDS micelles, DANTE water presaturation was used to eliminate the residual water signal. Chemical shifts were referenced to the solvent chemical shift (DMSO-*d*<sub>5</sub> (<sup>1</sup>H) 2.49 ppm or HOD 4.65 ppm).

**Conformation Analysis.** All the interproton-distance restraints between non-*J*-coupled protons are derived from the NOESY experiment. Seven interproton restraints shown in Figure 2 were classified into two categories. Upper bounds were fixed at 3.3 and 4.5 Å for strong and weak NOESY correlations, respectively, and a lower bound was fixed at 1.8 Å. Conformations were calculated using the MacroModel software version 8.6<sup>36</sup> installed on RedHat Linux 8 OS. Initial atomic coordinates and structure files were generated from the crystal data of *N*-iodoacetyl AmB.<sup>17</sup> The macrolide ring was treated as a semirigid group, in which ±30° allowance from the crystal structure was given to each C–C single bond upon calculations. The nonbonded van der Waals' interactions were represented by a simple repulsive quadratic term. The experimental distance restraints were represented as a soft asymptotic potential, and electrostatic interactions were ignored. The sampling of the conformational space was performed following a

(35) States, D. J.; Haberkorn, R. A.; Ruben, D. J. *J. Magn. Reson.* **1982**, *48*, 286–292.

(36) Mohamadi, F.; Richards, N. G.; Guida, W. C.; Liskamp, R.; Lipton, M.; Canfield, C.; Chang, G.; Hendrickson, T.; Still, W. C. *J. Comput. Chem.* **1990**, *11*, 440–467.

Monte Carlo Multiple Minimum method.<sup>37</sup> The MMFF force field<sup>38</sup> implemented in MacroModel was used, and 1000 random conformers were generated and minimized by the conjugate gradient method. A continuum solvation model using a generalized Born-surface area (GB/SA) method<sup>39</sup> was applied for water through the calculation.

**Measurement of Relaxation Induced by Mn<sup>2+</sup>.** A D<sub>2</sub>O solution of MnCl<sub>2</sub> was added to the micelle suspension so as to set the final concentration of MnCl<sub>2</sub> at 30 μM. Spin–lattice relaxation times  $T_1$  were determined using a standard 180–τ–90 inversion recovery pulse sequence with 10 τ values between 0.1 and 12 s. Measurements were performed at 30 °C in the presence and absence of Mn<sup>2+</sup>.

**Measurements of Self-Diffusion Coefficients.** For diffusion measurements, 4.5 mM AmB and 72 mM SDS (nondeuterated) were suspended in D<sub>2</sub>O. Diffusion coefficients were measured using a stimulated spin echo (STE) sequence.<sup>22</sup> The PFG-STE spectra were measured using a 500 MHz spectrometer equipped with a pulsed-field gradient unit. A 5 mm Nalorac inverse probe with an actively shielded z-gradient coil was used. The coil constant was calibrated with β-cyclodextrin, which has a diffusion coefficient of  $3.23 \times 10^{-10} \text{ m}^2 \text{ s}^{-1}$ .<sup>40</sup> In the PFG-STE experiment,<sup>22</sup> the attenuation of the NMR resonance depends on gradient area as shown in the following equation

$$I = I_0 \exp[-D(\Delta - \delta/3)\gamma^2 g^2 \delta^2]$$

where  $I_0$  is the intensity of the resonance in the NMR spectrum in the absence of gradient pulses,  $\gamma$  is the gyromagnetic ratio,  $\Delta$  is the time period during which diffusion occurs,  $g$  and  $\delta$  are the amplitude and duration of the bipolar gradient pulse pair, respec-

tively, and  $D$  is the self-diffusion coefficient. A series of 15 <sup>1</sup>H spectra were collected with the PFG-STE pulse sequence as a function of gradient amplitude. The gradient duration time,  $\delta$ , was 1 ms, the gradient amplitude was varied from 3.4 to 16.8 G cm<sup>-1</sup>, and the diffusion delay time,  $\Delta$ , was 5 s. All of the diffusion measurements were performed at 25 °C to compare the reported diffusion coefficient of SDS micelle.<sup>24</sup> After data acquisition, each free-induction decay was apodized with 1 Hz line broadening. Methyl protons at C12 of SDS were integrated and the peak integrals were plotted against the gradient pulse amplitude  $g$ , and the resultant plots were fitted to the above equation by using Origin 6.1 software to give the diffusion coefficient,  $D$  (see Figure S11 in the Supporting Information for the fitting curves). The methyl protons of SDS have a resonance at 0.8 ppm, where no AmB signal exists. In addition, since we used nondeuterated SDS at the molar ratio 15 times higher than AmB, we could almost ignore the influence of AmB signals on the diffusion experiments.

**CD Spectroscopy.** CD spectra were recorded with a 10-mm cuvette. A repetitive scanning of five cycles was used. Since the critical micelle concentration of SDS is approximately 8 mM,<sup>28</sup> concentrations of AmB and SDS were set to 0.5 mM and 8 mM, respectively.

**Acknowledgment.** We are grateful to Prof. Takahiro Sato for use of a CD spectrometer, Prof. Tohru Oishi in our laboratory for invaluable discussions, and Mr. Seiji Adachi in our department for assistance with the NMR measurements. This work was supported by Grants-In-Aid for Scientific Research (Nos. 15201048 and 18101010) and for Young Scientists (B) (No. 14780458) from MEXT, Japan.

**Supporting Information Available:** NMR spectra of AmB in SDS micelles and fitting curves for diffusion experiments. This material is available free of charge via the Internet at <http://pubs.acs.org>.

JO061309P

(37) Kolossvary, I.; Guida, W. C. *J. Comput. Chem.* **1999**, *20*, 1671–1684.

(38) Halgren, T. A. *J. Comput. Chem.* **1999**, *20*, 730–748.

(39) Still, W. C.; Tempczyk, A.; Hawley, R. C.; Hendrickson, T. *J. Am. Chem. Soc.* **1990**, *112*, 6127–6129.

(40) Uedaira, H.; Uedaira, H. *J. Phys. Chem.* **1970**, *74*, 2211–2214.